



**HAL**  
open science

# Comparison of automatic segmentation versus visual assessment of white matter hyperintensities and parenchymal atrophy in Alzheimer's disease

Lison Malaureille

► **To cite this version:**

Lison Malaureille. Comparison of automatic segmentation versus visual assessment of white matter hyperintensities and parenchymal atrophy in Alzheimer's disease. Human health and pathology. 2018. dumas-01887452

**HAL Id: dumas-01887452**

**<https://dumas.ccsd.cnrs.fr/dumas-01887452v1>**

Submitted on 8 Oct 2018

**HAL** is a multi-disciplinary open access archive for the deposit and dissemination of scientific research documents, whether they are published or not. The documents may come from teaching and research institutions in France or abroad, or from public or private research centers.

L'archive ouverte pluridisciplinaire **HAL**, est destinée au dépôt et à la diffusion de documents scientifiques de niveau recherche, publiés ou non, émanant des établissements d'enseignement et de recherche français ou étrangers, des laboratoires publics ou privés.



## AVERTISSEMENT

Ce document est le fruit d'un long travail approuvé par le jury de soutenance et mis à disposition de l'ensemble de la communauté universitaire élargie.

Il n'a pas été réévalué depuis la date de soutenance.

Il est soumis à la propriété intellectuelle de l'auteur. Ceci implique une obligation de citation et de référencement lors de l'utilisation de ce document.

D'autre part, toute contrefaçon, plagiat, reproduction illicite encourt une poursuite pénale.

Contact au SID de Grenoble :  
[bump-theses@univ-grenoble-alpes.fr](mailto:bump-theses@univ-grenoble-alpes.fr)

## LIENS

Code de la Propriété Intellectuelle. articles L 122. 4

Code de la Propriété Intellectuelle. articles L 335.2- L 335.10

<http://www.cfcopies.com/juridique/droit-auteur>

<http://www.culture.gouv.fr/culture/infos-pratiques/droits/protection.htm>



UNIVERSITÉ GRENOBLE ALPES  
UFR DE MÉDECINE DE GRENOBLE

Année: 2018

**COMPARISON OF AUTOMATIC SEGMENTATION VERSUS VISUAL  
ASSESSMENT OF WHITE MATTER HYPERINTENSITIES AND PARENCHYMAL  
ATROPHY IN ALZHEIMER'S DISEASE**

THÈSE

PRÉSENTÉE POUR L'OBTENTION DU TITRE DE DOCTEUR EN MÉDECINE

DIPLÔME D'ÉTAT

Mme Lison MALAUREILLE

[Données à caractère personnel]

THÈSE SOUTENUE PUBLIQUEMENT À LA FACULTÉ DE MÉDECINE DE GRENOBLE

Le : 27/09/2018

DEVANT LE JURY COMPOSÉ DE

Président du jury :

M le Professeur Alexandre KRAINIK (directeur de thèse)

Membres :

Mme le Docteur Sylvie GRAND

M le Professeur Alexandre MOREAU-GAUDRY

M le Docteur Olivier MOREAUD

*L'UFR de Médecine de Grenoble n'entend donner aucune approbation ni improbation aux opinions émises dans les thèses ; ces opinions sont considérées comme propres à leurs auteurs.*

Doyen de la Faculté : Pr. Patrice MORAND

Année 2017-2018

ENSEIGNANTS A L'UFR DE MEDECINE

CORPS	NOM-PRENOM	Discipline universitaire
PU-PH	ALBALADEJO Pierre	Anesthésiologie réanimation
PU-PH	APTEL Florent	Ophthalmologie
PU-PH	ARVIEUX-BARTHELEMY Catherine	Chirurgie générale
PU-PH	BAILLET Athan	Rhumatologie
PU-PH	BARONE-ROCHETTE Gilles	Cardiologie
PU-PH	BAYAT Sam	Physiologie
PU-PH	BENHAMOU Pierre Yves	Endocrinologie, diabète et maladies métaboliques
PU-PH	BERGER François	Biologie cellulaire
MCU-PH	BIDART-COUTTON Marie	Biologie cellulaire
MCU-PH	BOISSET Sandrine	Agents infectieux
PU-PH	BONAZ Bruno	Gastro-entérologie, hépatologie, addictologie
PU-PH	BONNETERRE Vincent	Médecine et santé au travail
PU-PH	BOREL Anne-Laure	Endocrinologie, diabète et maladies métaboliques
PU-PH	BOSSON Jean-Luc	Biostatistiques, informatique médicale et technologies de communication
MCU-PH	BOTTARI Serge	Biologie cellulaire
PU-PH	BOUGEROL Thierry	Psychiatrie d'adultes
PU-PH	BOUILLET Laurence	Médecine interne
PU-PH	BOUZAT Pierre	Réanimation
MCU-PH	BRENIER-PINCHART Marie Pierre	Parasitologie et mycologie
PU-PH	BRICAULT Ivan	Radiologie et imagerie médicale
PU-PH	BRICHON Pierre-Yves	Chirurgie thoracique et cardio- vasculaire
MCU-PH	BRIOT Raphaël	Thérapeutique, médecine d'urgence
MCU-PH	BROUILLET Sophie	Biologie et médecine du développement et de la reproduction
PU-PH	CAHN Jean-Yves	Hématologie
PU-PH	CARPENTIER Françoise	Thérapeutique, médecine d'urgence
PU-PH	CARPENTIER Patrick	Chirurgie vasculaire, médecine vasculaire
PU-PH	CESBRON Jean-Yves	Immunologie
PU-PH	CHABARDES Stephan	Neurochirurgie
PU-PH	CHABRE Olivier	Endocrinologie, diabète et maladies métaboliques
PU-PH	CHAFFANJON Philippe	Anatomie
PU-PH	CHARLES Julie	Dermatologie
PU-PH	CHAVANON Olivier	Chirurgie thoracique et cardio- vasculaire
PU-PH	CHIQUET Christophe	Ophthalmologie

PU-PH	CHIRICA Mircea	Chirurgie générale
PU-PH	CINQUIN Philippe	Biostatistiques, informatique médicale et technologies de communication
MCU-PH	CLAVARINO Giovanna	Immunologie
PU-PH	COHEN Olivier	Biostatistiques, informatique médicale et technologies de communication
PU-PH	COURVOISIER Aurélien	Chirurgie infantile
PU-PH	COUTURIER Pascal	Gériatrie et biologie du vieillissement
PU-PH	CRACOWSKI Jean-Luc	Pharmacologie fondamentale, pharmacologie clinique
PU-PH	CURE Hervé	Oncologie
PU-PH	DEBILLON Thierry	Pédiatrie
PU-PH	DECAENS Thomas	Gastro-entérologie, Hépatologie
PU-PH	DEMATTEIS Maurice	Addictologie
MCU-PH	DERANSART Colin	Physiologie
PU-PH	DESCOTES Jean-Luc	Urologie
MCU-PH	DETANTE Olivier	Neurologie
MCU-PH	DIETERICH Klaus	Génétique et procréation
MCU-PH	DOUTRELEAU Stéphane	Physiologie
MCU-PH	DUMESTRE-PERARD Chantal	Immunologie
PU-PH	EPAULARD Olivier	Maladies Infectieuses et Tropicales
PU-PH	ESTEVE François	Biophysique et médecine nucléaire
MCU-PH	EYSSERIC Hélène	Médecine légale et droit de la santé
PU-PH	FAGRET Daniel	Biophysique et médecine nucléaire
PU-PH	FAUCHERON Jean-Luc	Chirurgie générale
MCU-PH	FAURE Julien	Biochimie et biologie moléculaire
PU-PH	FERRETTI Gilbert	Radiologie et imagerie médicale
PU-PH	FEUERSTEIN Claude	Physiologie
PU-PH	FONTAINE Éric	Nutrition
PU-PH	FRANCOIS Patrice	Epidémiologie, économie de la santé et prévention
MCU-MG	GABOREAU Yoann	Médecine Générale
PU-PH	GARBAN Frédéric	Hématologie, transfusion
PU-PH	GAUDIN Philippe	Rhumatologie
PU-PH	GAVAZZI Gaétan	Gériatrie et biologie du vieillissement
PU-PH	GAY Emmanuel	Neurochirurgie
MCU-PH	GILLOIS Pierre	Biostatistiques, informatique médicale et technologies de communication
MCU-PH	GRAND Sylvie	Radiologie et imagerie médicale
PU-PH	GRIFFET Jacques	Chirurgie infantile
PU-PH	GUEBRE-EGZIABHER Fitsum	Néphrologie
MCU-PH	GUZUN Rita	Endocrinologie, diabétologie, nutrition, éducation thérapeutique
PU-PH	HAINAUT Pierre	Biochimie, biologie moléculaire
PU-PH	HENNEBICQ Sylviane	Génétique et procréation
PU-PH	HOFFMANN Pascale	Gynécologie obstétrique
PU-PH	HOMMEL Marc	Neurologie
PU-MG	IMBERT Patrick	Médecine Générale
PU-PH	JOUK Pierre-Simon	Génétique
PU-PH	JUVIN Robert	Rhumatologie

PU-PH	KAHANE Philippe	Physiologie
MCU-PH	KASTLER Adrian	Radiologie et imagerie médicale
PU-PH	KRACK Paul	Neurologie
PU-PH	KRAINIK Alexandre	Radiologie et imagerie médicale
PU-PH	LABARERE José	Epidémiologie ; Eco. de la Santé
MCU-PH	LABLANCHE Sandrine	Endocrinologie, diabète et maladies métaboliques
MCU-PH	LANDELLE Caroline	Bactériologie - virologie
MCU-PH	LAPORTE François	Biochimie et biologie moléculaire
MCU-PH	LARDY Bernard	Biochimie et biologie moléculaire
MCU-PH	LARRAT Sylvie	Bactériologie, virologie
MCU - PH	LE PISSART Audrey	Biochimie et biologie moléculaire
PU-PH	LECCIA Marie-Thérèse	Dermato-vénérologie
PU-PH	LEROUX Dominique	Génétique
PU-PH	LEROY Vincent	Gastro-entérologie, hépatologie, addictologie
PU-PH	LEVY Patrick	Physiologie
PU-PH	LONG Jean-Alexandre	Urologie
PU-PH	MAGNE Jean-Luc	Chirurgie vasculaire
MCU-PH	MAIGNAN Maxime	Thérapeutique, médecine d'urgence
PU-PH	MAITRE Anne	Médecine et santé au travail
MCU-PH	MALLARET Marie-Reine	Epidémiologie, économie de la santé et prévention
MCU-PH	MARLU Raphaël	Hématologie, transfusion
MCU-PH	MAUBON Danièle	Parasitologie et mycologie
PU-PH	MAURIN Max	Bactériologie - virologie
MCU-PH	MC LEER Anne	Cytologie et histologie
PU-PH	MERLOZ Philippe	Chirurgie orthopédique et traumatologie
PU-PH	MORAND Patrice	Bactériologie - virologie
PU-PH	MOREAU-GAUDRY Alexandre	Biostatistiques, informatique médicale et technologies de communication
PU-PH	MORO Elena	Neurologie
PU-PH	MORO-SIBILOT Denis	Pneumologie
PU-PH	MOUSSEAU Mireille	Cancérologie
PU-PH	MOUTET François	Chirurgie plastique, reconstructrice et esthétique ; brûlologie
MCU-PH	PACLET Marie-Hélène	Biochimie et biologie moléculaire
PU-PH	PALOMBI Olivier	Anatomie
PU-PH	PARK Sophie	Hémato - transfusion
PU-PH	PASSAGGIA Jean-Guy	Anatomie
PU-PH	PAYEN DE LA GARANDERIE Jean-François	Anesthésiologie réanimation
MCU-PH	PAYSANT François	Médecine légale et droit de la santé
MCU-PH	PELLETIER Laurent	Biologie cellulaire
PU-PH	PELLOUX Hervé	Parasitologie et mycologie
PU-PH	PEPIN Jean-Louis	Physiologie
PU-PH	PERENNOU Dominique	Médecine physique et de réadaptation
PU-PH	PERNOD Gilles	Médecine vasculaire
PU-PH	PIOLAT Christian	Chirurgie infantile
PU-PH	PISON Christophe	Pneumologie

PU-PH	PLANTAZ Dominique	Pédiatrie
PU-PH	POIGNARD Pascal	Virologie
PU-PH	POLACK Benoît	Hématologie
PU-PH	POLOSAN Mircea	Psychiatrie d'adultes
PU-PH	PONS Jean-Claude	Gynécologie obstétrique
PU-PH	RAMBEAUD Jacques	Urologie
PU-PH	RAY Pierre	Biologie et médecine du développement et de la reproduction
PU-PH	REYT Émile	Oto-rhino-laryngologie
PU-PH	RIGHINI Christian	Oto-rhino-laryngologie
PU-PH	ROMANET Jean Paul	Ophthalmologie
PU-PH	ROSTAING Lionel	Néphrologie
MCU-PH	ROUSTIT Matthieu	Pharmacologie fondamentale, pharmaco clinique, addictologie
MCU-PH	ROUX-BUISSON Nathalie	Biochimie, toxicologie et pharmacologie
MCU-PH	RUBIO Amandine	Pédiatrie
PU-PH	SARAGAGLIA Dominique	Chirurgie orthopédique et traumatologie
MCU-PH	SATRE Véronique	Génétique
PU-PH	SAUDOU Frédéric	Biologie Cellulaire
PU-PH	SCHMERBER Sébastien	Oto-rhino-laryngologie
PU-PH	SCHWEBEL-CANALI Carole	Réanimation médicale
PU-PH	SCOLAN Virginie	Médecine légale et droit de la santé
MCU-PH	SEIGNEURIN Arnaud	Epidémiologie, économie de la santé et prévention
PU-PH	STAHL Jean-Paul	Maladies infectieuses, maladies tropicales
PU-PH	STANKE Françoise	Pharmacologie fondamentale
MCU-PH	STASIA Marie-José	Biochimie et biologie moléculaire
PU-PH	STURM Nathalie	Anatomie et cytologie pathologiques
PU-PH	TAMISIER Renaud	Physiologie
PU-PH	TERZI Nicolas	Réanimation
MCU-PH	TOFFART Anne-Claire	Pneumologie
PU-PH	TONETTI Jérôme	Chirurgie orthopédique et traumatologie
PU-PH	TOUSSAINT Bertrand	Biochimie et biologie moléculaire
PU-PH	VANZETTO Gérald	Cardiologie
PU-PH	VUILLEZ Jean-Philippe	Biophysique et médecine nucléaire
PU-PH	WEIL Georges	Epidémiologie, économie de la santé et prévention
PU-PH	ZAOUI Philippe	Néphrologie
PU-PH	ZARSKI Jean-Pierre	Gastro-entérologie, hépatologie, addictologie

**PU-PH** : Professeur des Universités et Praticiens Hospitaliers  
**MCU-PH** : Maître de Conférences des Universités et Praticiens Hospitaliers  
**PU-MG** : Professeur des Universités de Médecine Générale  
**MCU-MG** : Maître de Conférences des Universités de Médecine Générale

## Table des matières

<i>Rappels</i> .....	8
<i>Résumé</i> .....	11
<i>Abstract</i> .....	13
<i>Introduction</i> .....	14
<i>Patients and Methods</i> .....	16
<b>Patients</b> .....	16
<b>MRI data acquisition</b> .....	16
<b>MRI data analysis</b> .....	17
A. White matter hyperintensities analysis.....	17
B. Parenchymal atrophy .....	19
<i>Results</i> .....	23
<b>Patients' characteristics</b> .....	23
<b>White matter analysis</b> .....	24
A. Visual assessment.....	24
B. Automated segmentation.....	24
C. Comparison .....	25
<b>Parenchymal atrophy</b> .....	26
A. Visual assessment.....	26
B. Automated segmentation.....	26
C. Comparison .....	27
<i>Discussion</i> .....	29
<b>White Matter Hyperintensities</b> .....	29
<b>Parenchymal atrophy</b> .....	30
A. Hippocampal atrophy.....	30
B. Frontal and Parietal atrophy.....	31
<b>Relationship between WMH and parenchymal atrophy</b> .....	32
<b>Limitations of the study</b> .....	33
<i>Conclusion</i> .....	34
<i>References</i> .....	35



*Conclusion signée*..... 39  
*Serment d'Hippocrate* ..... 41

## Rappels

La maladie d'Alzheimer représente plus de 70 % de l'ensemble des démences de la personne âgée.

La démence se définit (selon le DSM IV) par une atteinte des fonctions intellectuelles et cognitives. Sa sévérité entraîne une perte d'autonomie dans les gestes de la vie quotidienne ou dans les interactions sociales. Les troubles doivent évoluer depuis six mois au minimum.

Une entité clinique intermédiaire entre le vieillissement physiologique et la démence a été défini par le terme : Troubles Cognitifs Légers amnésiques (TCL-A). Il s'agit d'un syndrome défini par un déclin cognitif plus important que celui que l'on s'attend à trouver à un âge et niveau d'éducation donnés, mais qui n'a pas de retentissement sur les activités de la vie quotidienne.

Des tests neuropsychologiques sont réalisés chez les patients suspects de démence. Le test le plus important dans la maladie d'Alzheimer est le test de Gröber & Buschke, ou test du Rappel libre/Rappel indicé à 16 items (RL/RI-16).

Le test est composé de 16 mots appartenant à 16 catégories sémantiques différentes et comprend successivement une phase de contrôle de l'encodage, un rappel indicé immédiat, trois essais successifs de rappels libre et indicé, une phase de rappels libre et indicé différés (20 minutes), suivie par une phase de reconnaissance.

Il permet d'évaluer la présence et la nature des difficultés de mémoire épisodique verbale.

La maladie d'Alzheimer est caractérisée par deux types de lésions, les lésions amyloïdes et les lésions tau ou dégénérescences neuro-fibrillaires. Si le patient présente ces deux sortes de lésions, alors le diagnostic de maladie d'Alzheimer certaine peut être posé.

Des tests paracliniques sont réalisés afin de rechercher indirectement la présence de ces lésions. Une ponction lombaire permet de rechercher un taux de peptide A $\beta$ 1-42 bas et des taux de protéine Tau totale et phosphorylée élevés. Une scintigraphie (ou PET-scan) cérébrale à l'amyloïde permet d'évaluer la densité des plaques. En cas de début précoce, avec ou sans antécédents familiaux de maladie d'Alzheimer, la recherche de mutations autosomiques dominantes sur les gènes *APP*, *PSEN1* et *PSEN2* peut également être réalisée.

Les critères diagnostics pour la maladie d'Alzheimer typique ont récemment évolué en 2014, et ils reposent sur l'association :

- D'un phénotype clinique spécifique évoluant graduellement et progressivement depuis 6 mois et correspondant à un syndrome amnésique de type hippocampique
- Et de critères physiopathologiques de la maladie d'Alzheimer sur les résultats de la ponction lombaire, du PET-TDM ou des analyses génétiques.

Une imagerie cérébrale systématique est recommandée pour tout trouble cognitif avéré de découverte récente (recommandations HAS). Le but de cet examen est :

- D'éliminer une cause curable (tumeur cérébrale, infection cérébrale, hydrocéphalie à pression normale) ou de rechercher des images séquellaires (traumatiques, vasculaires).
- D'objectiver une atrophie associée ou non à des lésions vasculaires afin d'orienter vers une maladie neurodégénérative ou une démence vasculaire.

Cet examen est une imagerie par résonance magnétique nucléaire (IRM) avec des séquences T1, T2, T2\* et FLAIR et des coupes coronales permettant de visualiser l'hippocampe. À défaut une tomodensitométrie cérébrale est réalisée.

Les processus dégénératifs et vasculaires co-existent fréquemment dans les démences.

Il n'existe actuellement aucun traitement pour guérir ou même modifier l'évolution anatomopathologique de la maladie d'Alzheimer. En revanche, il existe des traitements qui ont pour but de traiter certains symptômes du malade sans empêcher la progression de la maladie (inhibiteurs de l'acétylcholinestérase et la Mémantine qui bloque les récepteurs NMDA).

Un diagnostic précoce est important pour débiter au plus tôt les traitements médicamenteux actuels, mais également tous les conseils préconisés en matière de prévention, stimuler au mieux les facultés cognitives et de mémorisation. Il permet aussi au malade de prendre des dispositions pour l'avenir tant qu'il possède encore ses facultés de discernement et de prise de décision et pour sa famille, d'anticiper la perte d'autonomie avec la mise en place progressive d'aides au domicile.

## Résumé

**Introduction** : Les hyper intensités de la substance blanche et l'atrophie du parenchyme cérébral sont des anomalies courantes chez les patients âgés et les patients atteints de démence. Les logiciels de segmentation automatique pourraient être utiles pour l'analyse des patients adressés pour des troubles cognitifs légers amnésiques (TCLa) ou une maladie d'Alzheimer (MA) probable.

**Patients et méthodes** : 123 patients pris en charge pour des TCLa ou une MA probable ont été examinés par IRM (2D Axial Flair, 3DT1 FFE). Les volumes normalisés des hyper signaux de la substance blanche et des épaisseurs corticales ont été mesurés grâce aux logiciels Pixyl.neuro et FreeSurfer puis comparés aux scores visuels habituels.

**Résultats** : 110 sur 123 patients (89%) ont été analysés après exclusion d'examens pour des problèmes techniques ou des erreurs de segmentation. Les volumes des hyper intensités de la substance blanche étaient corrélés aux scores visuels de Fazekas ( $r=0.78$ ). Les volumes hippocampiques étaient corrélés aux scores visuels de Scheltens ( $r>0.63$ ). Par contre, les volumes d'épaisseurs corticales frontales et pariétales n'étaient pas corrélés aux scores visuels d'atrophie pariétale ni au gradient d'atrophie fronto-pariétale.

**Conclusion** : Les analyses de segmentation automatique sont fiables pour évaluer les hyper intensités de la substance blanche et les volumes hippocampiques, tels que visuellement estimés. En revanche, la segmentation corticale automatique ne permet pas de mesurer l'atrophie fronto-pariétale telle qu'elle est couramment évaluée dans la pratique clinique.

# **Comparison of automatic segmentation versus visual assessment of white matter hyperintensities and parenchymal atrophy in Alzheimer's disease**

Lison Malaureille<sup>1</sup>, Felix Renard<sup>2</sup>, Alan Tucholka<sup>3</sup>, Maud Medici<sup>4</sup>, Alexandre Krainik<sup>1,2,5,6</sup>

*<sup>1</sup>Department of Neuroradiology, University Hospital of Grenoble, France*

*<sup>2</sup>IRMaGe facility, University Grenoble Alpes, France, France*

*<sup>3</sup>Pixyl, Grenoble, France*

*<sup>4</sup>CIT803, University Hospital of Grenoble, France*

*<sup>5</sup>University of Grenoble Alps, Grenoble, France*

*<sup>6</sup>Grenoble Institute of Neurosciences, Inserm, Grenoble, France*

## Abstract

**Introduction:** White matter hyperintensities (WMH) and parenchymal atrophy are common findings in elderly and in dementia. Automated segmentation could be helpful for quantification in patients referred for amnesic Mild Cognitive Impairment (aMCI) and probable Alzheimer's disease (AD).

**Methods:** 123 patients referred for probable AD or aMCI had a MRI (Axial Flair, 3D T1-FFE). Normalized WMH and cortical volumes were measured using Pixyl.neuro and FreeSurfer and compared to usual visual scores.

**Results:** 110 out of 123 patients (89%) were analyzed after exclusion because of technical issues or inaccurate segmentation. WMH volumes were correlated with Fazekas' visual scores ( $r=0.78$ ). Hippocampal volumes were correlated with Scheltens' visual scores ( $r>0.63$ ). However frontal and parietal cortical volumes were not correlated with visual scores of parietal atrophy and the gradient of frontoparietal atrophy.

**Conclusion:** Automated segmentations are reliable to estimate WMH and hippocampal volumes, as visually assessed. However, automated cortical segmentation does not allow to classify frontoparietal atrophy as routinely performed in clinical practice.

## Introduction

Alzheimer's disease (AD) is the most common cause of dementia, affecting over 46 million people worldwide, and may grow up to 131.5 million by 2050.

According to new IWG-2 and NIA-AA criteria for AD, magnetic resonance imaging (MRI) is necessary for the identification of comorbidity or non-AD conditions and to characterize the clinical phenotype (1).

In clinical practice, morphological brain imaging rules out other causes of dementia, evaluates the severity of microangiopathy (2,3) and may strengthen the diagnosis of AD by assessing the hippocampal atrophy (4) and the medial temporal atrophy, which is the best MRI marker at a prodromal stage of further progression (1,5).

Hippocampal atrophy is now a widely accepted marker of AD (1,6,7). Visual assessment is commonly used in clinical practice with a good reliability (8), even when compared to automatic segmentation (6). Hippocampal atrophy is correlated with both tau deposition and episodic memory deficit (9). However, it has a low specificity. Indeed, hippocampal atrophy is present in other dementias such as fronto-temporal lobar degeneration, and even normal ageing (10,11).

To better characterize cerebral structural abnormalities and improve diagnosis performances, MRI may also provide additional features of the brain degeneration, such as parietal atrophy (8,12,13) and microangiopathy (3). It has been established that cortical thinning is related with white matter intensities (14,15), even though the relation is not well known.

AD dementia is an anatomically heterogeneous disease and several patterns were identified (8,16).

Using these additional imaging biomarkers among patients suspected of AD and MCI with severe hippocampal atrophy, subgroups were identified. Some patients had a predominant parietal atrophy without significant microangiopathy. Others had a significant microangiopa-



thy without predominant parietal atrophy. Interestingly, subtle changes in executive functions and memory impairment were identified across groups (8).

All of these results were based on MRI visual rating.

When analyzing structural MRI, differences among inter- and intra-rater agreements were identified depending on brain imaging experience and parameters (6,8). Computer-based methods were proposed to provide volumetric quantification to assist the diagnosis, including classification algorithms that may improve diagnosis performance, especially in less experienced radiologists (17,18).

Automated cortical thickness measurements are often used to assess gray matter changes and several software such as FreeSurfer or Cat 12 are reliable (19,20).

Yet, there is no consensus for an automated method for quantitative assessment of white matter hyperintensities (WMH) on magnetic resonance imaging and a few have been studied (21).

The objectives of this retrospective study on patients with AD and amnesic Mild Cognitive Impairment (MCI) aimed to: i) estimate the relationships between quantitative measures of regional cortical thinning and WMH with visual rating, ii) assess morphological heterogeneity among patients and identify subgroups, iii) characterize neuropsychological impairment for each subgroup.

## **Patients and Methods**

### **Patients**

We included 123 patients who initially met either diagnostic criteria for probable AD of the NIA-AA (7) or the research criteria for aMCI due to AD (22).

Demographics data included age, sex, and education level. Factors of cardiovascular risk were also identified, including diabetes, hypertension, dyslipidemia, smoking, and personal history of vascular disease.

Exclusion criteria were default MRI acquisition and inappropriate segmentation.

Among these patients, twelve patients had spinal tap to confirm the diagnosis with positive biomarkers.

Seventy-four patients had neuropsychological tests in a lap time of 6 months around the MRI.

Our standardized neuropsychological battery contained tests for attention, language, praxis, parietal function, visuoconstructive function, verbal and visual memory, working memory, and frontal executive function. The neuropsychological tests were the visual memory part of Signoret battery for mnesic efficiency (BEM 84) (23), 16-item free and cued recall (24): RL/RI-16, including the third immediate free and total recall scores, delayed free and total recall scores, verbal intrusions score, yes/no recognition performance; forward and backward digit span (25), the difference between forward and backward digit span, ideo-motor and constructive praxis, Bachy test (26), Trail Making Test (TMT) A and B (27), semantic and alphabetic fluency (28), a composite executive score; visuospatial and visuoperceptive tests (29).

The institutional review board approved the research protocol on 19 May 2014, IRB 5891.

### **MRI data acquisition**

All examinations were performed on a Philips 1.5T (n=72) or 3T MRI (n=51) (ACHIEVA, Philips Healthcare, the Netherlands), with the following protocol: T2-WI (3 mm) coronal slic-

es orthogonal to the hippocampus, axial FLAIR (4 mm), axial T2\*-WI (4 mm), 3D-GRE T1-WI (1×1×1 mm). All data were anonymized.

## **MRI data analysis**

### **A. White matter hyperintensities analysis**

#### *1) Visual assessment*

We retrieved visual scores previously published by Chapuis *et al.* (8), namely the microangiopathy according to the modified Fazekas's score, ranging from 0 (no WMH) to 3 (extensive WMH) (2). Examinations were blindly rated twice by five raters: 1 senior neuroradiologist; 1 senior neurologist; 1 junior neurologist; 2 residents in neuroradiology. Median values of all these scores were used. For each score, median values were multiplied by 2 to keep integers. Intra- and interrater agreements were previously detailed (8).

#### *2) Automated segmentation*

We used an original software called Pixyl.Neuro ([www.pixylmedical.com](http://www.pixylmedical.com), Pixyl SA, Grenoble, France).

Both T1-weighted and FLAIR images are first brain-extracted using ANTs (30), denoised (31), and corrected for intensity inhomogeneities using the N4 algorithm (32). Prior anatomical information is introduced into the analysis by means of a brain template and associated tissue probabilistic maps that are non-linearly registered to the subject T1 space. The T1-weighted image is co-registered to the FLAIR image using an affine transform. A weighted multi-sequence Markov model (33) is then used to perform the segmentation of normal tissues. This algorithm also produces a weight map that indicates how well each voxel fits the model and can therefore be used to identify atypical regions. These candidate lesion voxels

are then extracted and processed through a set of post-processing filters to retain only voxels that correspond to characteristic WMH lesion traits.

Segmentation is illustrated in Figure 1.

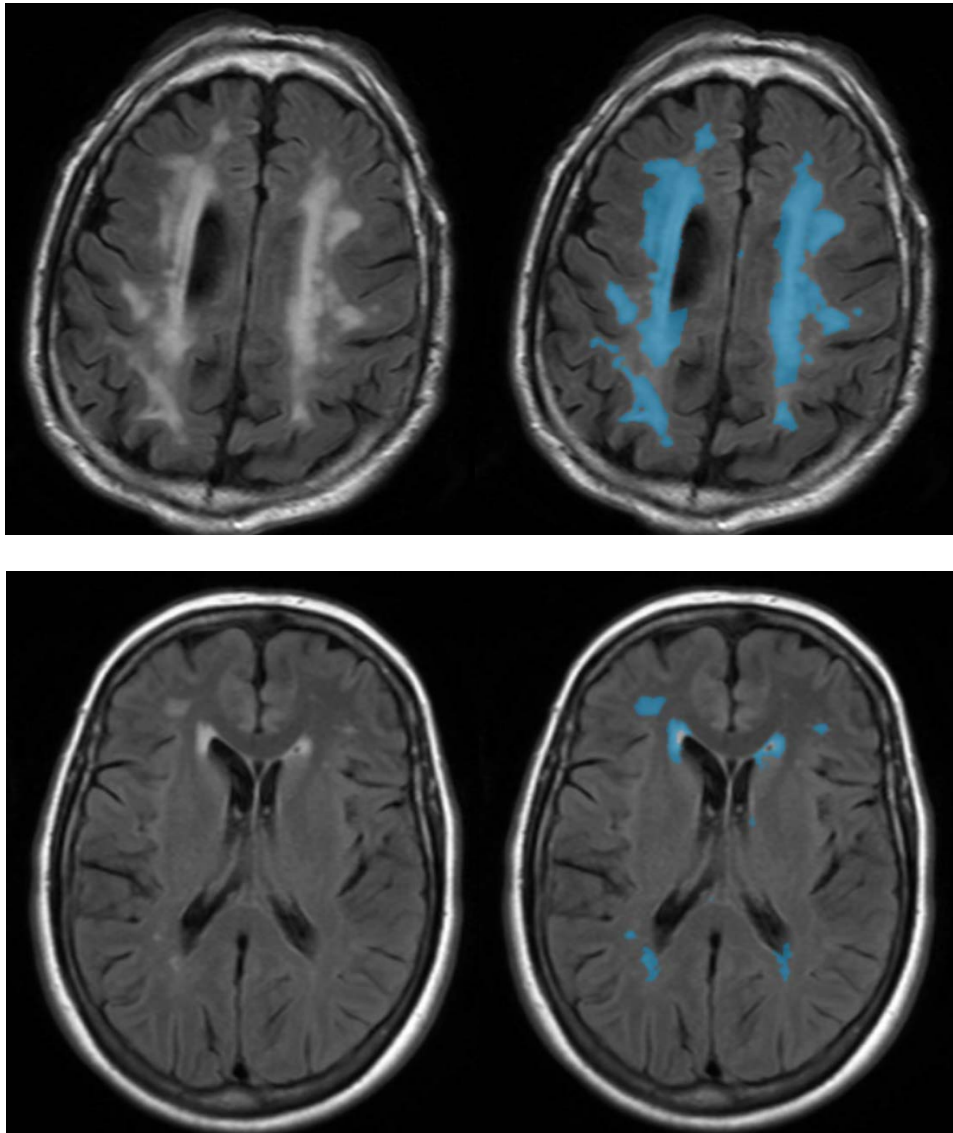


**Figure 1 : White matter hyperintensities segmentation with Pixyl.neuro – Left Slices correspond to native images; On right slices, blue masks correspond to automated segmentation.**

All segmented WMH were visually analyzed to check the quality of segmentation.

Individual segmented lesional volumes were normalized by the intracranial volumes.

### 3) *Statistical comparisons*

Statistical analyses were performed using R software (version  $\geq 3.4.1$ ). A correlation analysis was conducted to test the correlation between WMH volumes and Fazekas' scores.

#### B. Parenchymal atrophy

##### 1) *Visual assessment*

We retrieved the different visual scores previously published by Chapuis *et al.* (8):

- the hippocampal atrophy according to Scheltens' score, ranging from 0 (no atrophy) to 4 (severe atrophy) (4);
- the parietal atrophy (PA) according to the visual rating score for posterior cortical atrophy, ranging from 0 (no atrophy) to 3 (severe atrophy) (12);
- the gradient of frontoparietal atrophy (GFPA) based on anteroposterior enlargement of the medial sulci of the frontal and parietal lobes ranging from -2 (anterior enlargement) to +3 (posterior enlargement) (8) The GFPA has been proposed to easily assess the selective lobar atrophy, and especially the precuneal atrophy onto parasagittal views.

Again, median values were used and multiplied by 2 to keep integers, as previously described above.

## 2) *Automated segmentation*

We used FreeSurfer to measure cortical atrophy.

The surface-based pipeline consists of several stages (described in detail in (34,35)). First, the volume is registered with the MNI305 (36) atlas (this is an affine registration). This allows FreeSurfer to compute seed points in later stages. The B1 bias field is estimated by measuring the variation in the white matter intensity. The main body of the white matter is used to estimate the field across the entire volume. Likely white matter points are chosen based on their locations in MNI305 space as well as on their intensity and the local neighborhood intensities. The intensity at each voxel is then divided by the estimated bias field at that location in order to remove the effect of the bias field. The skull is stripped (Figure 2A; (37)) using a deformable template model. Voxels are then classified as white matter or something other than white matter (Figure 2B) based on intensity and neighbor constraints. Cutting planes are chosen to separate the hemispheres from each other as well as to remove the cerebellum and brain stem. The location of the cutting planes is based on the expected MNI305 location of the corpus callosum and pons, as well as several rules-based algorithms that encode the expected shape of these structures. An initial surface is then generated for each hemisphere by tiling the outside of the white matter mass for that hemisphere. This initial surface is then refined to follow the intensity gradients between the white and gray matter (this is referred to as the white surface). The white surface is then nudged to follow the intensity gradients between the gray matter and CSF (this is the pial surface). The white and pial surfaces overlaid on the original T1 weighed image are shown in Figure 2C. The distance between the white and the pial gives us the thickness at each location of cortex (38).

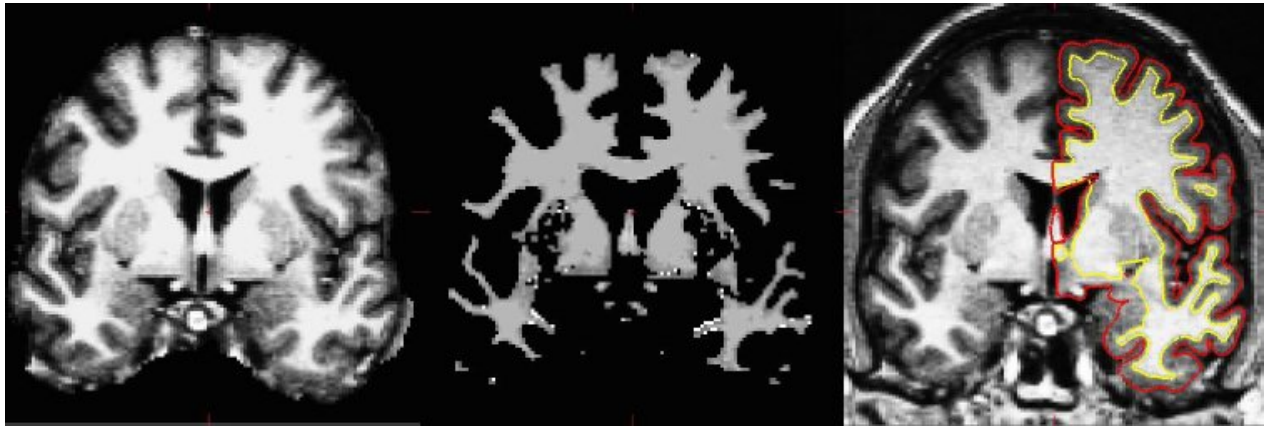


Figure 2 Three stages from the FreeSurfer cortical analysis pipeline. A. skull stripped image. B. white matter segmentation. C. surface between white and gray (yellow line) and between gray and pia (red line) overlaid on the original volume.

Freesurfer provided the normalized cortical thickness of 74 labels per hemisphere (sulcus or gyri).

Segmentation is illustrated in Figure 3.

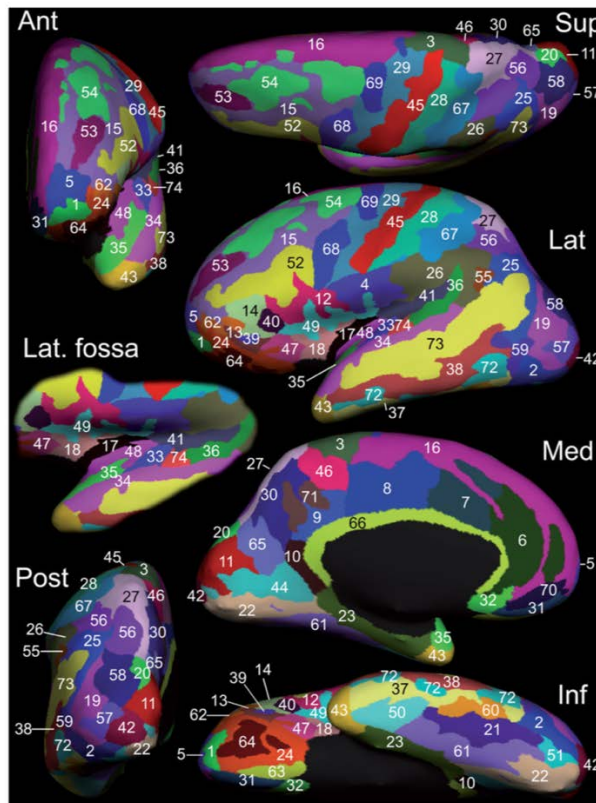


Figure 3 : Inflated view of the manual parcellation of one hemisphere of the Training set (39)

A visual verification of the automated segmentation was performed by a five-year trained radiologist.

### 3) *Statistical comparisons*

We conducted correlation analyses to evaluate the relationships between qualitative and quantitative measurements.

**Hippocampal atrophy:** we compared for each hemisphere Scheltens' scores to the automated and normalized hippocampal volumes.

**Parietal atrophy:** we compared, for each hemisphere, the parietal atrophy visual rating score to: successively: precuneus label - the mean of cortical thickness of precuneus, superior parietal lobule, supramarginal gyrus and postcentral gyrus - and the mean of cortical thickness of every parietal label.

**GFPA:** we compared, for each hemisphere, the GFPA's scores to successively: - the difference between the cortical thickness of precuneus and superior frontal gyrus - the difference between the mean of cortical thickness of precuneus, superior parietal lobule, supramarginal gyrus and postcentral gyrus and the mean of cortical thickness of superior frontal gyrus, middle frontal gyrus and precentral gyrus, and finally the difference between the mean of cortical thickness of every frontal label and the mean of cortical thickness of every parietal label.



## Results

### Patients' characteristics

Among the 123 selected patients, 13 patients were excluded because of:

1. Default acquisition: Coronal T2 instead of Axial Flair images (n=1)
2. Pixyl.neuro software's technical issues (n=4)
3. Inappropriate segmentation
  - Erroneous Pyxil.neuro segmentation (n=7) due to inclusion of intra-orbital fat or cortical bone
  - Erroneous Freesurfer segmentation (n=1)

It left 110 patients to study.

Among those, 66 examinations were performed on 1.5T (60%) and 44 exams on 3T MR scan (40%).

There were 23 aMCI (20.9 %) and 87 AD patients (79.1 %), 67 women (60.9 %) and 43 men (39.1 %). The mean age was 76 years +/- 8 (53 - 89 years).

Cardiovascular disease risk factors, age, sex, and education level did not differ between patients who underwent neuropsychological testing or not.

Neuropsychological results are summarized in Table 1.

<b>Test</b>	<b>Range</b>	<b>Median</b>
MMS (/30)	7 - 30	23
Encoding (/16)	5 - 16	14
Third immediate free call scores (/16)	0 - 13	5
Third immediate total recall scores (/16)	0 - 16	13
Delayed free recall scores (/16)	0 - 15	5
Delayed total recall scores (/16)	2- 16	13
Intrusions (%)	0 - 67	6
Recognitions (/16)	0 - 16	15

**Table 1: Patients neuropsychological main characteristics**

## **White matter analysis**

### **A. Visual assessment**

The median value of visual assessment's scores was 2. Median values were multiplied by two to keep integer, so it corresponds to a score of 1 on Fazekas' score, that is mild microangiopathy.

### **B. Automated segmentation**

White matter analysis provided the volume of brain microangiopathy lesions. Mean volume was  $17.63 \pm 15.7$  ml (0.98-88 ml). Mean normalized volume with the total intracranial volume was  $1.2 \pm 1.0\%$  (0.1-5.8%).

### C. Comparison

The correlation analysis was performed twice. First, we tested the effect of MRI strength on lesional volumes. No difference was detected. Thus, we disregarded this parameter for WMH analysis.

Results are illustrated in Figure 4.

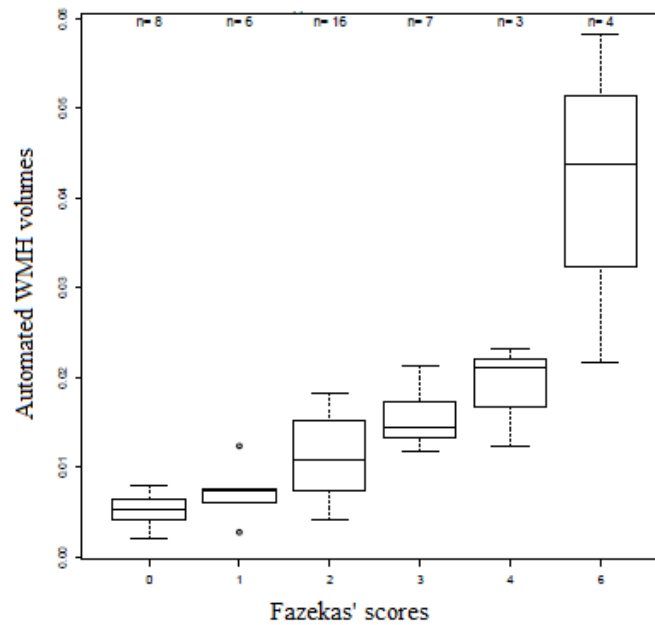


**Figure 4: Comparison between automated WMH volumes and Fazekas' scores - Correlation coefficient = 0.78**

There is a very good correlation between the lesional volumes and the Fazekas' scores (correlation coefficient Pearson  $r = 0.78$ ;  $p < 0.001$ ).

## **Parenchymal atrophy**

### **A. Visual assessment**

The median value of hippocampal visual assessment's score was 5 on both right and left side.

The median value was multiplied by two to keep integer. It corresponds to a mild to moderate hippocampal atrophy.

The median value of parietal atrophy according to the visual rating score for posterior cortical atrophy was 3 on both right and left side. The median value was multiplied by two to keep integer. It corresponds to a minimal to moderate parietal atrophy.

The median value of visual assessment of frontoparietal atrophy was 2 on each side. Again, the median value was multiplied by two to keep integer. It corresponds to a mild posterior enlargement.

### **B. Automated segmentation**

The automated segmentation provided cortical thicknesses of the 74 regions of interest, for each hemisphere, that is 148 values for each patient, normalized with total intracranial volumes.

Mean normalized cortical thickness was  $0.7 \pm 0.6\%$  (0.0017-4.5%).

### C. Comparison

The correlation analysis was performed twice. First, we tested the effect of MRI strength on lesional volumes. No difference was detected. Thus, we disregarded this parameter for WMH analysis.

Results are detailed in Figure 5.

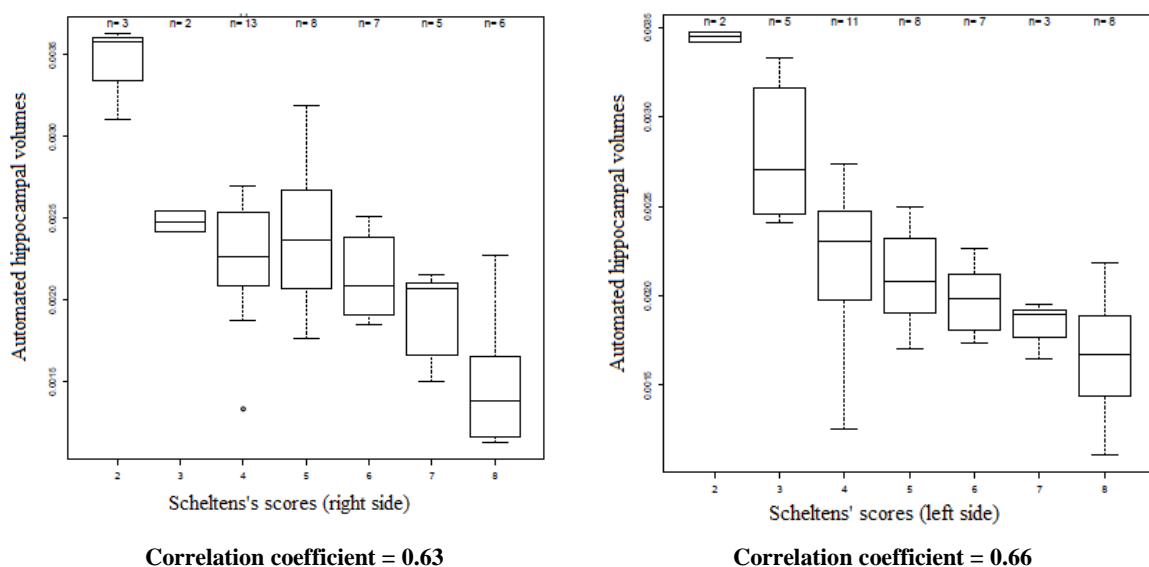


**Figure 5: Comparison between automated hippocampal volumes and Scheltens' scores visually assessed**

*Hippocampal atrophy* - There is a good correlation between the hippocampal volumes and Scheltens' scores, with correlation coefficient Pearson  $r = 0.66$ ;  $p < 0.001$  on the left side, and correlation coefficient Pearson  $r = 0.63$ ;  $p < 0.001$  on the right side.

*Parietal atrophy* - There is no significant correlation between the cortical thicknesses and the parietal atrophy visual rating score in both hemispheres, either using precuneus label, the 4 major labels in parietal lobe or all the labels in parietal lobe: correlation coefficient Pearson  $r = 0.24, 0.27$  and  $0.3$  respectively on the left side ( $p > 0.05$ ); correlation coefficient Pearson  $r = 0.12, 0.05$  and  $0.05$  respectively on the right side ( $p > 0.05$ ).

*GFPA* - There is no significant correlation between the cortical thicknesses in frontal and parietal lobes and the score based on anteroposterior enlargement of the medial sulci of the frontal and parietal lobes, in both hemisphere, either using single labels, major labels in parietal and frontal lobes or using all the labels in parietal and frontal lobes: correlation coefficient Pearson  $r = 0.2, 0.24$  and  $0.38$  respectively on the left side ( $p > 0.05$ ); correlation coefficient Pearson  $r = 0.15, 0.18$  and  $0.18$  respectively on the right side ( $p > 0.05$ ).

## **Discussion**

Imaging plays an important role in dementia. Indeed, brain imaging is highly recommended to conduct etiological inquiry. Besides intracranial diseases that require neurosurgical treatment, stroke, and neurological involvement in infectious, inflammatory or metabolic diseases, brain imaging may help to identify markers of neurodegenerative diseases such as AD. Among those, WMH, hippocampal atrophy and parietal atrophy are currently visually evaluated. In the recent years, several softwares were proposed to better quantify these markers. Moreover, computerized based evaluation may help to identify pathological profiles and provide more accurate evaluations. It could help to accelerate the diagnosis process. An early diagnosis would allow an early treatment and would benefit the patient. Here, we compared automated segmentation and visual assessments in patients referred for aMCI and probable AD. We showed that automated segmentation is in line with visual evaluation of WHM and hippocampal atrophy. However, automated cortical segmentation was not appropriate to estimate frontal and parietal parenchymal atrophy as visually assessed.

## **White Matter Hyperintensities**

WMH are detected on T2/FLAIR-WI in cognitively normal subjects, MCI, AD, and other conditions. WMH burden is associated to cardiovascular risk factors that have to be diagnosed and cared. WMH patterns may help to identify small cerebral arteries diseases such arteriolosclerosis related to chronic arterial hypertension and CADASIL. Its clinical relevance has been debated but several studies showed its cognitive impact. Indeed, WMH burden is associated with memory impairment in AD (40) and predictive of a faster decline of global functioning in non-disabled older patients (2). A systematic review and meta-analysis provides strong evidence that white matter hyperintensities predict the risk of stroke, dementia, and mortality (41).

Our study is consistent with previous works, showing a very good correlation between automatic segmentation and Fazekas' scores (42). Here, we used a new original software that brings support for rapid diagnosis on large population. Seven patients had to be excluded after visual verification because of erroneous segmentation with orbital-fat or cortical bone inclusion. This was due to thick slices. Pixyl.neuro usually analyses 3mm-thickness slices. In our work, Flair sequences consisted in 4-mm-thickness slices, resulting with an inaccurate registration of T1-weighted images to Flair and partial volume effect in about 5% of cases. Visual check of the 110 patients revealed that Pyxil.neuro segmentation tends to slightly overestimate WMH size. Despite this bias related to partial volume effect on 2D FLAIR images, lesional volumes were correlated with Fazekas's score.

Now, WMH evaluation ought to be performed using 3D FLAIR images instead of 2D images (43). Indeed, thinner slices with improved signal to noise ratio, improved CSF and flow saturation help to better identify WMH. Thus, improved automatic WMH segmentation is expected when using 3D Flair images (44).

## **Parenchymal atrophy**

### **A. Hippocampal atrophy**

Hippocampal atrophy is a sensitive but specific marker of AD (4). When present and in case of clinical suspicion, it helps to advocate for AD (8,45). Thus, It also has been suggested that MRI-based hippocampal volume measurement could be helpful to monitor AD progression (45). Our study is in line with previous work which showed that hippocampal analysis was helpful for differential diagnosis among healthy normal controls, MCI, and AD (46). This was based on a combination of volumetry, cortical thickness, hippocampal shape, and hippocampal texture extracted from single T1-weighted structural MRI only. It revealed that hippo-



campal texture was the most important feature in the algorithm followed by hippocampal volume, ventricular volume, and parietal lobe thickness.

Consistent with previous works (47,48), our study showed good correlation between automatic segmented hippocampal volume and Scheltens' scores. Indeed, previous studies showed that Freesurfer reported larger hippocampal volume than manual tracing, but it still allows an accurate classification according to the degree of atrophy (0, 1, 2, 3 or 4 on Scheltens' score).

## B. Frontal and Parietal atrophy

Besides hippocampal atrophy, additional regional atrophy is helpful to better diagnose neurodegenerative diseases. Indeed, parietal atrophy alone or when compared to frontal atrophy such as in gradient of frontoparietal atrophy were identified in AD (8,12). Additionally, parietal atrophy and WMH rating allowed to identify cognitive subgroups among patients with probable AD (8). We chose FreeSurfer because the cortical thickness measurements allowed to classify subjects in subgroups of healthy elderly, MCI, and AD (49).

Here, cortical segmentation using FreeSurfer could not help to retrieve subjective parietal atrophy visual classifications. This result is not in line with a large multicenter study of pathologically proven dementias (50) which demonstrated that visual rating scores (Medial Temporal, Anterior Cingulate, Orbito-Frontal, Anterior Temporal, Fronto-Insula, Posterior) from routinely acquired structural MRIs were correlated with cerebral atrophy using voxel-based morphometry (50). Among major differences with our study on AD and patients at risk, this study was conducted among heterogeneous demented patients, including Lewy bodies disease, early-onset AD, late-onset AD, frontotemporal lobar degeneration, and cognitively normal control subjects. Moreover, we used individual values of regional cortical thickness instead of averaged gray matter density as estimated by voxel-based morphometry. To our point

of view, our approach is closer to clinical practice based on individual results instead of groups comparisons.

These results are important, illustrating the limits of automatic cortical segmentation. Indeed, visual rating of regional cerebral atrophy is mainly based on the visual assessment of enlarged subarachnoid spaces related to both white and grey matter atrophy rather than cortical atrophy alone. It could be proposed to segment regional CSF spaces instead of cortical thickness in order to retrieve the visual sub-groups.

### **Relationship between WMH and parenchymal atrophy**

The relationship between white matter and grey matter lesions is not clearly understood yet.

The second objective of this work was to study the relationship between WMH and cortical atrophy using automated segmentation. Previously, we identified within the same population subgroups of patients (8). Indeed, we observed that the WMH burden was inversely related to the severity of the parietal atrophy. Causal relationships between these 2 markers are unclear. Indeed, it seems unlikely that a disease responsible of parietal atrophy would protect against the occurrence of WMH. Inversely, it also seems very unlikely that WMH may protect against the occurrence of parietal atrophy.

In fact, the occurrence of WMH is associated with cerebral atrophy in healthy (51) and in Alzheimer's subjects (40,52).

Jacobs in 2014 (15) described a negative correlation between WMH and frontal cortical thinning in AD but a positive correlation (higher level of WMH volume associated with higher cortical thickness) in parietal lobes and in frontal lobes for MCI.

Other studies showed that microangiopathy was inversely associated with cortical thinning in the precuneus and superior parietal regions (14) or that WMH in AD is not associated with

medial temporal lobe atrophy, but PWMH is independently correlated with hippocampal volume reduction (53).

It reveals relationship between WMH and grey matter loss is definitely not uncovered yet. Automated analysis could not allow to retrieve the different morphological profiles and we didn't succeed to find a significant association between WMH and cortical thinning.

In several study, deep WMH and periventricular WMH (PWMH) were differentiated, due to probably different origins (14,52,53) which is something we could do in forthcoming study.

### **Limitations of the study**

The main limitations of this study were the lack pathophysiological marker of AD such as CSF analysis or amyloid PET (1). This was due to a poor acceptance of spinal TAP in the study group and a local difficulty to access to PET imaging at the time of the study. However, most patients presented typical clinical phenotypes after 5 years of medical follow-up and 12 patients presented with positive CSF biomarkers. We chose to use a different cohort from ADNI (Alzheimer's Disease Neuroimaging Initiative) subjects to corroborate our findings. A prospective study, integrating positive CSF biomarkers or amyloid PET, could verify our findings.

The interest into molecular biomarkers is considerable (1,54) because there is a lot at stake for an early AD's diagnosis and potential early treatment. But classification accuracy on MRI visual rating scores in the diagnosis of dementia has been shown to be comparable to the accuracy of the CSF beta-amyloid ( $A\beta_{1-42}$ ) (50,55). Imaging is a crucial milestone in early AD diagnosis, particularly with automated analysis.

Number of studies demonstrated the interest, that could be very important in the future, of computerized method (6,17,20). But a considerable issue is that automated analyses require long and sophisticated post-processing. This limits its application in daily practice and for

some clinicians leads to the will of doing without it (56,57). It can be argued that this area will see prompt and substantial progress in the future allowing a routinely use of these post-imaging analyses.

## **Conclusion**

Automated analysis is close to visual analysis for microangiopathy and hippocampal atrophy. But automatically measured cortical atrophy was not correlated with visually assessed frontal and parietal atrophy. It does not allow to retrieve the visually assessed clinical and radiological different profiles among AD and aMCI patients. Accelerating AD diagnosis means a very significant scientific improvement and it may be presumed that there will be room for automated analysis, maybe with innovative software that measures regional white matter and CSF volumes in addition to grey matter volume. These could be very interesting tools for radiologists in the future to reduce intra- and interrater variability, to better quantify abnormalities in order to improve diagnosis and therapeutic monitoring.

## References

1. Dubois B, Feldman HH, Jacova C, Hampel H, Molinuevo JL, Blennow K, et al. Advancing research diagnostic criteria for Alzheimer's disease: the IWG-2 criteria. *Lancet Neurol.* juin 2014;13(6):614-29.
2. Inzitari D, Pracucci G, Poggesi A, Carlucci G, Barkhof F, Chabriat H, et al. Changes in white matter as determinant of global functional decline in older independent outpatients: three year follow-up of LADIS (leukoaraiosis and disability) study cohort. *BMJ.* 6 juill 2009;339(jul06 1):b2477-b2477.
3. Prins ND, Scheltens P. White matter hyperintensities, cognitive impairment and dementia: an update. *Nat Rev Neurol.* mars 2015;11(3):157-65.
4. Scheltens P, Leys D, Barkhof F, Huglo D, Weinstein HC, Vermersch P, et al. Atrophy of medial temporal lobes on MRI in « probable » Alzheimer's disease and normal ageing: diagnostic value and neuropsychological correlates. *J Neurol Neurosurg Psychiatry.* 1 oct 1992;55(10):967-72.
5. Risacher SL, Saykin AJ, West JD, Shen L, Firpi HA, McDonald BC. Baseline MRI Predictors of Conversion from MCI to Probable AD in the ADNI Cohort. :16.
6. And the Alzheimer's Disease Neuroimaging Initiative, Boutet C, Chupin M, Colliot O, Sarazin M, Mutlu G, et al. Is radiological evaluation as good as computer-based volumetry to assess hippocampal atrophy in Alzheimer's disease? *Neuroradiology.* déc 2012;54(12):1321-30.
7. McKhann GM, Knopman DS, Chertkow H, Hyman BT, Jack CR, Kawas CH, et al. The diagnosis of dementia due to Alzheimer's disease: Recommendations from the National Institute on Aging-Alzheimer's Association workgroups on diagnostic guidelines for Alzheimer's disease. *Alzheimers Dement.* mai 2011;7(3):263-9.
8. Chapuis P, Sauvée M, Medici M, Serra A, Banciu E, Moreau-Gaudry A, et al. Morphologic and neuropsychological patterns in patients suffering from Alzheimer's disease. *Neuroradiology.* mai 2016;58(5):459-66.
9. Frisoni GB, Fox NC, Jack CR, Scheltens P, Thompson PM. The clinical use of structural MRI in Alzheimer disease. *Nat Rev Neurol.* févr 2010;6(2):67-77.
10. Laakso MP, Partanen K, Riekkinen P, Lehtovirta M, Helkala E-L, Hallikainen M, et al. Hippocampal volumes in Alzheimer's disease, Parkinson's disease with and without dementia, and in vascular dementia: An MRI study. *Neurology.* 1 mars 1996;46(3):678-81.
11. Du A-T, Schuff N, Kramer JH, Rosen HJ, Gorno-Tempini ML, Rankin K, et al. Different regional patterns of cortical thinning in Alzheimer's disease and frontotemporal dementia. *Brain.* 21 nov 2006;130(4):1159-66.
12. Koedam ELGE, Lehmann M, van der Flier WM, Scheltens P, Pijnenburg YAL, Fox N, et al. Visual assessment of posterior atrophy development of a MRI rating scale. *Eur Radiol.* déc 2011;21(12):2618-25.
13. From the Imaging Cognitive Impairment Network (ICINET), Wahlund L-O, Westman E, van Westen D, Wallin A, Shams S, et al. Imaging biomarkers of dementia: recommended visual rating scales with teaching cases. *Insights Imaging.* févr 2017;8(1):79-90.
14. Seo SW, Lee J-M, Im K, Park J-S, Kim S-H, Kim ST, et al. Cortical thinning related to periventricular and deep white matter hyperintensities. *Neurobiol Aging.* juill 2012;33(7):1156-1167.e1.
15. Jacobs HIL, Clerx L, Gronenschild EHBM, Aalten P, Verhey FRJ. White Matter Hyperintensities are Positively Associated with Cortical Thickness in Alzheimer's Disease. *J Alzheimers Dis.* 24 janv 2014;39(2):409-22.
16. Noh Y, Jeon S, Lee JM, Seo SW, Kim GH, Cho H, et al. Anatomical heterogeneity of

Alzheimer disease: Based on cortical thickness on MRIs. *Neurology*. 18 nov 2014;83(21):1936-44.

17. Schmitter D, Roche A, Maréchal B, Ribes D, Abdulkadir A, Bach-Cuadra M, et al. An evaluation of volume-based morphometry for prediction of mild cognitive impairment and Alzheimer's disease. *NeuroImage Clin*. 2015;7:7- 17.
18. Kloppel S, Stonnington CM, Chu C, Draganski B, Scahill RI, Rohrer JD, et al. Automatic classification of MR scans in Alzheimer's disease. *Brain*. 7 févr 2008;131(3):681- 9.
19. Seiger R, Ganger S, Kranz GS, Hahn A, Lanzenberger R. Cortical Thickness Estimations of FreeSurfer and the CAT12 Toolbox in Patients with Alzheimer's Disease and Healthy Controls: Cortical Thickness of FreeSurfer and CAT12. *J Neuroimaging* [Internet]. 15 mai 2018 [cité 3 août 2018]; Disponible sur: <http://doi.wiley.com/10.1111/jon.12521>
20. Möller C, Pijnenburg YAL, van der Flier WM, Versteeg A, Tijms B, de Munck JC, et al. Alzheimer Disease and Behavioral Variant Frontotemporal Dementia: Automatic Classification Based on Cortical Atrophy for Single-Subject Diagnosis. *Radiology*. juin 2016;279(3):838- 48.
21. Caligiuri ME, Perrotta P, Augimeri A, Rocca F, Quattrone A, Cherubini A. Automatic Detection of White Matter Hyperintensities in Healthy Aging and Pathology Using Magnetic Resonance Imaging: A Review. *Neuroinformatics*. juill 2015;13(3):261- 76.
22. Albert MS, DeKosky ST, Dickson D, Dubois B, Feldman HH, Fox NC, et al. The diagnosis of mild cognitive impairment due to Alzheimer's disease: Recommendations from the National Institute on Aging-Alzheimer's Association workgroups on diagnostic guidelines for Alzheimer's disease. *Alzheimers Dement*. mai 2011;7(3):270- 9.
23. Signoret J-L. BEM 144: Batterie d'efficience mnésique 144. Fond. IPSEN Paris Elsevier Collect. Esprit Cerveau. 1991;
24. Grober E, Buschke H, Crystal H, Bang S, Dresner. Screening for dementia by memory testing. *Neurology*. juin 1988;38(6):900-3.
25. Monaco M, Costa A, Caltagirone C, Carlesimo GA. Forward and backward span for verbal and visuo-spatial data: standardization and normative data from an Italian adult population. *Neurol Sci*. mai 2013;34(5):749- 54.
26. Bachy-Languedoc. Batterie d'examen des troubles en dénomination. Brux. Ed. 1989;
27. Ashendorf L, Jefferson A, Oconnor M, Chaisson C, Green R, Stern R. Trail Making Test errors in normal aging, mild cognitive impairment, and dementia. *Arch Clin Neuropsychol* [Internet]. 21 févr 2008 [cité 4 sept 2018]; Disponible sur: <https://academic.oup.com/acn/article-lookup/doi/10.1016/j.acn.2007.11.005>
28. Carlesimo GA, Caltagirone C, Gainotti G, Fadda L, Gallassi R, Lorusso S, et al. The Mental Deterioration Battery: Normative Data, Diagnostic Reliability and Qualitative Analyses of Cognitive Impairment. *Eur Neurol*. 1996;36(6):378- 84.
29. Herrera-Guzmán I, Peña-Casanova J, Lara JP, Gudayol-Ferré E, Böhm P. Influence of Age, Sex, and Education on the Visual Object and Space Perception Battery (VOSP) In a Healthy Normal Elderly Population. *Clin Neuropsychol*. janv 2004;18(3):385- 94.
30. Avants BB, Tustison NJ, Song G, Cook PA, Klein A, Gee JC. A reproducible evaluation of ANTs similarity metric performance in brain image registration. *NeuroImage*. févr 2011;54(3):2033- 44.
31. Manjón JV, Coupé P, Martí-Bonmatí L, Collins DL, Robles M. Adaptive non-local means denoising of MR images with spatially varying noise levels: Spatially Adaptive Non-local Denoising. *J Magn Reson Imaging*. janv 2010;31(1):192- 203.
32. Tustison NJ, Avants BB, Cook PA, Yuanjie Zheng, Egan A, Yushkevich PA, et al. N4ITK: Improved N3 Bias Correction. *IEEE Trans Med Imaging*. juin 2010;29(6):1310- 20.
33. Forbes F, Doyle S, Garcia-Lorenzo D, Barillot C, Dojat M. Adaptive weighted fusion of multiple MR sequences for brain lesion segmentation. In: 2010 IEEE International Sympo-

- sium on Biomedical Imaging: From Nano to Macro [Internet]. Rotterdam, Netherlands: IEEE; 2010 [cité 28 août 2018]. p. 69- 72. Disponible sur: <http://ieeexplore.ieee.org/document/5490413/>
34. Fischl B, Sereno MI, Dale AM. Cortical Surface-Based Analysis. :13.
  35. Dale AM, Fischl B, Sereno MI. Cortical Surface-Based Analysis. :16.
  36. Collins, DL, Neelin, P., Peters, TM, and Evans, AC. Automatic 3D Inter-Subject Registration of MR Volumetric Data in Standardized Talairach Space. *Journal of Computer Assisted Tomography*. 1994;18(2) p192-205, 1994 PMID: 8126267; UI: 94172121.
  37. Ségonne F, Dale AM, Busa E, Glessner M, Salat D, Hahn HK, et al. A Hybrid Approach to the Skull Stripping Problem in MRI. :32.
  38. Fischl B, Dale AM. Measuring the thickness of the human cerebral cortex from magnetic resonance images. *Proc Natl Acad Sci*. 26 sept 2000;97(20):11050- 5.
  39. Destrieux C, Fischl B, Dale A, Halgren E. Automatic parcellation of human cortical gyri and sulci using standard anatomical nomenclature. *NeuroImage*. oct 2010;53(1):1- 15.
  40. Capizzano AA. White matter hyperintensities are significantly associated with cortical atrophy in Alzheimer's disease. *J Neurol Neurosurg Psychiatry*. 1 juin 2004;75(6):822- 7.
  41. Debette S, Markus HS. The clinical importance of white matter hyperintensities on brain magnetic resonance imaging: systematic review and meta-analysis. *BMJ*. 26 juill 2010;341(jul26 1):c3666- c3666.
  42. Tsai J-Z, Peng S-J, Chen Y-W, Wang K-W, Li C-H, Wang J-Y, et al. Automated Segmentation and Quantification of White Matter Hyperintensities in Acute Ischemic Stroke Patients with Cerebral Infarction. *Minnerup J, éditeur. PLoS ONE*. 15 août 2014;9(8):e104011.
  43. Paniagua Bravo á, Sánchez Hernández JJ, Ibáñez Sanz L, Alba de Cáceres I, Crespo San José JL, García-Castaño Gandariaga B. A comparative MRI study for white matter hyperintensities detection: 2D-FLAIR, FSE PD 2D, 3D-FLAIR and FLAIR MIP. *Br J Radiol*. mars 2014;87(1035):20130360.
  44. Anbeek P, Vincken KL, van Bochove GS, van Osch MJP, van der Grond J. Probabilistic segmentation of brain tissue in MR imaging. *NeuroImage*. oct 2005;27(4):795- 804.
  45. Schröder J, Pantel J. Neuroimaging of hippocampal atrophy in early recognition of Alzheimer's disease – a critical appraisal after two decades of research. *Psychiatry Res Neuroimaging*. janv 2016;247:71- 8.
  46. Sørensen L, Igel C, Pai A, Balas I, Anker C, Lillholm M, et al. Differential diagnosis of mild cognitive impairment and Alzheimer's disease using structural MRI cortical thickness, hippocampal shape, hippocampal texture, and volumetry. *NeuroImage Clin*. 2017;13:470- 82.
  47. Schmidt MF, Storrs JM, Freeman KB, Jack CR, Turner ST, Griswold ME, et al. A comparison of manual tracing and FreeSurfer for estimating hippocampal volume over the adult lifespan. *Hum Brain Mapp*. juin 2018;39(6):2500- 13.
  48. Fraser MA, Shaw ME, Anstey KJ, Cherbuin N. Longitudinal Assessment of Hippocampal Atrophy in Midlife and Early Old Age: Contrasting Manual Tracing and Semi-automated Segmentation (FreeSurfer). *Brain Topogr [Internet]*. 4 juill 2018 [cité 3 août 2018]; Disponible sur: <http://link.springer.com/10.1007/s10548-018-0659-2>
  49. Chepkoech J-L, Walhovd KB, Grydeland H, Fjell AM, for the Alzheimer's Disease Neuroimaging Initiative. Effects of change in FreeSurfer version on classification accuracy of patients with Alzheimer's disease and mild cognitive impairment: Effects of Change in FreeSurfer Version. *Hum Brain Mapp*. mai 2016;37(5):1831- 41.
  50. Harper L, Fumagalli GG, Barkhof F, Scheltens P, O'Brien JT, Bouwman F, et al. MRI visual rating scales in the diagnosis of dementia: evaluation in 184 post-mortem confirmed cases. *Brain*. avr 2016;139(4):1211- 25.

51. Wen W, Sachdev PS, Chen X, Anstey K. Gray matter reduction is correlated with white matter hyperintensity volume: A voxel-based morphometric study in a large epidemiological sample. *NeuroImage*. févr 2006;29(4):1031- 9.
52. Ha S-Y, Youn YC, Kim S, Hsiung G-YR, Ahn S-W, Shin H-W, et al. A voxel-based morphometric study of cortical gray matter volume changes in Alzheimer's disease with white matter hyperintensities. *J Clin Neurosci*. nov 2012;19(11):1506- 10.
53. Jang J-W, Kim S, Na HY, Ahn S, Lee SJ, Kwak K-H, et al. Effect of White Matter Hyperintensity on Medial Temporal Lobe Atrophy in Alzheimer's Disease. *Eur Neurol*. 2013;69:229- 35.
54. Ahmed RM, Paterson RW, Warren JD, Zetterberg H, O'Brien JT, Fox NC, et al. Biomarkers in dementia: clinical utility and new directions. *J Neurol Neurosurg Psychiatry*. déc 2014;85(12):1426- 34.
55. Ewers M, Mattsson N, Minthon L, Molinuevo JL, Antonell A, Popp J, et al. CSF biomarkers for the differential diagnosis of Alzheimer's disease: A large-scale international multicenter study. *Alzheimers Dement*. nov 2015;11(11):1306- 15.
56. Shen Q, Loewenstein DA, Potter E, Zhao W, Appel J, Greig MT, et al. Volumetric and visual rating of magnetic resonance imaging scans in the diagnosis of amnesic mild cognitive impairment and Alzheimer's disease. *Alzheimers Dement*. juill 2011;7(4):e101- 8.
57. Davies RR, Scallan VL, Graham A, Williams GB, Graham KS, Hodges JR. Development of an MRI rating scale for multiple brain regions: comparison with volumetrics and with voxel-based morphometry. *Neuroradiology*. août 2009;51(8):491- 503.



## Conclusion signée

**THÈSE SOUTENUE PAR :** Lison MALAUREILLE

**TITRE :**

**COMPARISON OF AUTOMATIC SEGMENTATION VERSUS VISUAL ASSESSMENT  
OF WHITE MATTER HYPERINTENSITIES AND PARENCHYMAL ATROPHY IN  
ALZHEIMER'S DISEASE**

**CONCLUSION :**

Chez les patients pris en charge pour une Maladie d'Alzheimer (MA) probable et des troubles cognitifs légers amnésiques (TCLa), l'étude de la micro angiopathie et de l'atrophie encéphalique régionale a montré l'existence de sous-groupes cliniques et radiologiques.

Notre étude a pour objectif de comparer des logiciels de segmentation automatique à des scores visuels en évaluant les hyper intensités de la substance blanche et l'atrophie du parenchyme cérébral chez ces patients.

123 patients pris en charge pour des TCLa ou une MA probable par le centre mémoire de ressources et de recherche de Grenoble, ont été examinés par IRM 1.5T ou 3T (Séquences Axiales Flair, 3D T1-FFE) dans le service de Neuroradiologie du CHU de Grenoble entre 2008 et 2013. Les marqueurs de la maladie d'Alzheimer tels que la micro angiopathie et l'atrophie parenchymateuse ont été évalués par des logiciels de segmentation automatique. Ils ont ensuite été comparés avec les scores visuels habituels, en réalisant des analyses de corrélation.

110 patients ont pu être analysés après exclusion de treize examens en raison de problèmes techniques ou de défauts de segmentation, soit 89% des patients. Pour la micro angiopathie, les analyses statistiques ont montré qu'il existait une très bonne corrélation entre les volumes des hyper intensités de la substance blanche mesurés par le logiciel de segmentation et les scores de Fazekas ( $r=0.78$ ). Pour l'atrophie hippocampique, il existait une bonne corrélation entre les

scores automatiques et les scores visuels de Scheltens bilatéraux ( $r=0.66$  et  $r=0.63$ ). Pour l'atrophie parenchymateuse frontale et pariétale, il n'existait aucune corrélation entre les épaisseurs corticales mesurées par le logiciel de segmentation et l'atrophie évaluée visuellement par les scores d'atrophie pariétale et le gradient d'atrophie fronto-pariétale.

Les analyses de segmentation automatique sont fiables dans l'évaluation des hyper intensités de la substance blanche et de l'atrophie hippocampique. Ces données sont importantes compte-tenu de leur retentissement clinique et de leurs caractères étiologique et pronostique. En revanche, la mesure automatique de l'atrophie corticale n'était pas du tout corrélée aux scores d'atrophie frontale et pariétale du parenchyme cérébral évalués visuellement. Ces résultats suggèrent que les analyses visuelles d'atrophie parenchymateuse frontale et pariétale correspondent plutôt à une analyse de l'atrophie corticale et sous-corticale, par l'élargissement des espaces liquidiens péri-cérébraux, et non pas aux épaisseurs corticales, trop fines pour être analysées à l'œil nu. Par conséquent les différents groupes morphologiques n'ont pas pu être retrouvés. Des évolutions logicielles sont attendues pour retrouver les sous-groupes identifiés visuellement.

**VU ET PERMIS D'IMPRIMER**  
**Grenoble, le : 05/09/2018**


**LE DOYEN**



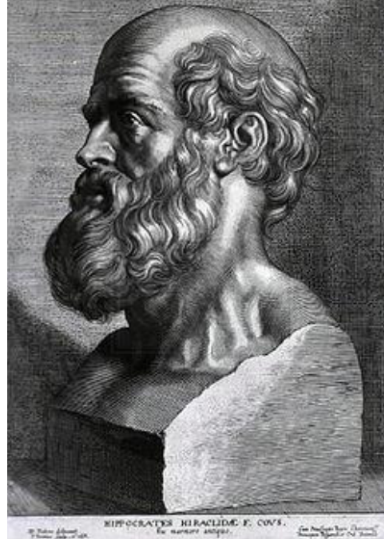
**Pr. Patrice MORAND**

**LE PRÉSIDENT DE LA THÈSE**

**Pr. Alexandre KRAINIK**



## Serment d'Hippocrate



### **SERMENT D'HIPPOCRATE**

*En présence des Maîtres de cette Faculté, de mes chers condisciples et devant l'effigie d'HIPPOCRATE,*

*Je promets et je jure d'être fidèle aux lois de l'honneur et de la probité dans l'exercice de la Médecine.*

*Je donnerai mes soins gratuitement à l'indigent et n'exigerai jamais un salaire au dessus de mon travail. Je ne participerai à aucun partage clandestin d'honoraires.*

*Admis dans l'intimité des maisons, mes yeux n'y verront pas ce qui s'y passe ; ma langue taira les secrets qui me seront confiés et mon état ne servira pas à corrompre les mœurs, ni à favoriser le crime.*

*Je ne permettrai pas que des considérations de religion, de nation, de race, de parti ou de classe sociale viennent s'interposer entre mon devoir et mon patient.*

*Je garderai le respect absolu de la vie humaine.*

*Même sous la menace, je n'admettrai pas de faire usage de mes connaissances médicales contre les lois de l'humanité.*

*Respectueux et reconnaissant envers mes Maîtres, je rendrai à leurs enfants l'instruction que j'ai reçue de leurs pères.*

*Que les hommes m'accordent leur estime si je suis fidèle à mes promesses.*

*Que je sois couvert d'opprobre et méprisé de mes confrères si j'y manque.*